Applied Mathematics & Information Sciences
An International Journal

http://dx.doi.org/10.12785/amis/080543

Operator based Robust Nonlinear Control Design to an Ionic Polymer Metal Composite with Uncertainties and Input Constraints

Aihui Wang[1,*], *Gong Wei*[2] *and Hui Wang*[1]

[1] School of Electronic Information, Zhongyuan University of Technology, Zhengzhou, 450007, China
[2] Department of Information Engineering, Henan Communication Vocational Technology College, Zhengzhou, 450052, China

Received: 15 Sep. 2013, Revised: 13 Dec. 2013, Accepted: 14 Dec. 2013
Published online: 1 Sep. 2014

Abstract: In this paper, robust nonlinear control design to an ionic polymer metal composite (IPMC) with uncertainties and input constraints is studied. The IPMC is a novel smart polymer material, and many potential applications for low mass high displacement actuators in biomedical and robotic systems have been shown. In general, the IPMC has highly nonlinear property, and the control input is subject to some constraints to ensure safety and longer service life of IPMC. Moreover, there exist uncertainties caused by identifying some physical parameters and approximate calculation in dynamic model. As a result, considering measurement error of parameters and model error, a practical nonlinear model is obtained, and a nonlinear robust control design with uncertainties and input constraints using operator-based robust right coprime factorization is proposed. The effectiveness of the proposed control method based on obtained nonlinear model is confirmed by simulation and experimental results.

Keywords: Ionic polymer metal composite, uncertainties, input constraints, robust nonlinear control, robust right coprime factorization.

1 Introduction

The ionic polymer metal composite (IPMC) belongs to the category electroactive polymers (EAP), which is one of the most promising EAP actuators for applications, also called artificial muscle, is being developed to enable effective, miniature, light and low power actuators. Because IPMCs have the following characteristics: large strain and stress induced electrically, light in weight, small and simple mechanisms, small electric consumption, and low drive voltage etc., which have been shown to have many potential applications for developments of miniature robots and biomedical devices [1,2].

The IPMC is usually broken up into three categories of different model types: black-box, gray-box, and white-box [3]. The black-box models have no prior knowledge of the system at all. The gray-box models have some knowledge of system or structure. The white-box models are obtained by physical system derivation and have a comprehensive knowledge of physics system. It can be said that most black-box and gray-box models were developed to study certain response characteristics or phenomena in the material, which are mainly linear models. The white-box models, on the other hand, attempt to model physical processes taking place within the actuator, which are usually nonlinear models. For linear models, linear quadratic regulator (LQR), proportional integral and derivative (PID), adaptive fuzzy algorithm and impedance control scheme have been designed in precise position control [4]. Moreover, the IPMC shows mainly nonlinear behaviors in characteristics of large strain and stress, and a practical mathematical model and an effective control method are desirable in precise position control.

Precision position control is critical in ensuring precise and safe operation of IPMC actuators. Considering an application as a robotic manipulator, IPMC has to move arbitrarily from one specified position to another. It needs a skilful operator to control manually based on his or her experiences to stop the swing immediately at the right position. It is well known that

* Corresponding author e-mail: wah781212@gmail.com

right coprime factorization has been a promising approach for analysis, design, stabilization and control of nonlinear system [5]. Especially, robust right coprime factorization has attracted much attention due to its convenient in researching input-output stability problems of nonlinear system [6,7,8,9]. On the whole, this approach has been proved effective in theoretical studies and practical applications on nonlinear systems. However, for nonlinear system with uncertainties and input constraints, how to realize output tracking performance is still a challenging issue. As a result, in this paper, robust nonlinear precision position control design to an IPMC with uncertainties and input constraints is studied. That is, first, considering measurement error of parameters and model error of IPMC, an improved practical nonlinear model with uncertainties of IPMC is obtained. Second, an operator-based robust nonlinear control design to IPMC with uncertainties and input constraints is presented. Finally, some simulation and experimental results are shown to confirm the effectiveness of the proposed control method based on obtained nonlinear model.

The outline of the paper is organized as follows. In Section **2**, an nonlinear model with uncertainties of IPMC and problem statement are described. Operator theorem are introduced, and robust stable control design using operator based approach is proposed in Section **3**. The simulation and experimental results are shown in Section **4**, and Section **5** is the conclusions.

2 Nonlinear model and problem statement

2.1 Nonlinear model of IPMC

The dynamic models of IPMCs fall into two general categories: linear models, and nonlinear models. Linear models have no prior knowledge or some knowledge of the system. Nonlinear models have a comprehensive knowledge of the physics system derivation. A nonlinear dynamic model of IPMC can be modeled by the following equations [3]:

$$\begin{cases} \dot{v} = -\frac{v+Y(v)(R_a+R_c)-u}{(C_1(v)+C_a(v))(R_a+R_c)} \\ y = \frac{3\alpha_0\kappa_e(\sqrt{2\Gamma(v)}-v)}{Y_e H^2} \end{cases} \tag{1}$$

where, v is the state variable, u is the control input voltage, y is the curvature output, R_a is the electrodes resistance, R_c is the ion diffusion resistance, α_0 is the coupling constant, Y_e is the equivalent Young's modulus of IPMC, and κ_e is the effective dielectric constant of the polymer. $\Gamma(v)$, $C_1(v)$ and $C_a(v)$ are functions of the state variable and some parameters,

$$\Gamma(v) = \frac{b}{a^2}\left(\frac{ave^{-av}}{1-e^{-av}} - ln\left(\frac{ave^{-av}}{1-e^{-av}}\right) - 1\right) \tag{2}$$

where,

$$\begin{cases} a = \frac{F(1-C^-\Delta V)}{RT} \\ b = \frac{F^2C^-(1-C^-\Delta V)}{RT\kappa_e} \end{cases} \tag{3}$$

F is Faraday's constant, C^- is the anion concentrations, ΔV is the volumetric change, R is the gas constant, and T is the absolute temperature.

$$C_1(v) = S\kappa_e\frac{\dot{\Gamma}(v)}{\sqrt{2\Gamma(v)}} \tag{4}$$

$S = WL$ is the surface area of the IPMC, L, W and H denote the length, the width and the thickness of the IPMC respectively.

$$C_a(v) = \frac{q_1SF}{RT}\frac{K_1C^{H^+}e^{-\frac{vF}{RT}}}{(K_1C^{H^+}+e^{-\frac{vF}{RT}})^2} \tag{5}$$

$K_1 = \frac{k_1}{k_{-1}}$, k_1 and k_{-1} are the chemical rate constants for forward and reverse directions of electrochemical surface process, q_1 is some constant, and C^{H+} is the concentration of the hydrion H^+.

$$Y(v) = Y_1v + Y_2v^2 + Y_3v^3 \tag{6}$$

Y_1, Y_2 and Y_3 are the coefficients of polynomial.

2.2 Problem Statement

The above dynamic model has a comprehensive knowledge of the physics system derivation, and is an accurate mathematical model. However, it is difficult to be adopted absolutely in practice because it is still difficult to identify accurately some physical parameters. Moreover, some physical parameters are small enough for influence of dynamic model. As a result, in this paper, a practical nonlinear model is obtained. In the following part of this subsection, how to obtain the practical nonlinear model based above dynamic model will be explained.

In general, ΔV is little enough in (3), and C^- is a bound constant, then $|C^-\Delta V| \to 0$, the parameters a and b in (3) can be calculated approximately by the following equations,

$$a \approx \frac{F}{RT}, \quad b \approx \frac{F^2C^-}{RT\kappa_e} \tag{7}$$

The IPMC can operate in a humid environment or a dry environment, in this paper, the IPMC setup is investigated in a dry environment, then $C^{H+} \to 0$, so

$$C_a(v) \approx 0 \tag{8}$$

In (6), Y_1, Y_2 and Y_3 are little enough, and $|Y(v)| \ll |v|$. So, in (1), because R_a and R_c are bounded, $Y(v)$ can be ignored and considered as model error. In addition to some physical constants, such as T, L, W, H, R_a, and R_c

must be measured or identified by experiments, which will also create error. Therefore, in this paper, a now nonlinear model is obtained,

$$\begin{cases} \dot{v} = -\frac{v-u}{C_1(v)(R_a+R_c)} \\ y = \frac{3\alpha_0\kappa_e\sqrt{2\Gamma(v)}}{Y_eH^2} + \Delta P \end{cases} \tag{9}$$

where, ΔP is uncertainties consisting of identifying error of parameters and model error of the IPMC.

Substituting (2), (4) and (7) into (9), the following nonlinear dynamic model of IPMC is obtained,

$$\begin{cases} \dot{v} = -\frac{(v-u)\sqrt{2b(\frac{ave^{-av}}{1-e^{-av}} - ln(\frac{ave^{-av}}{1-e^{-av}})-1)}}{S\kappa_e b(R_a+R_c)(1-\frac{1-e^{-av}}{ave^{-av}})\frac{e^{-av}(1-e^{-av}-av)}{(1-e^{-av})^2}} \\ y = \frac{3\alpha_0\kappa_e\sqrt{2b(\frac{ave^{-av}}{1-e^{-av}} - ln(\frac{ave^{-av}}{1-e^{-av}})-1)}}{aY_eH^2} + \Delta P \end{cases} \tag{10}$$

Defining a new state variable $x = av$, the above nonlinear dynamic model can also be described by the following equations,

$$\begin{cases} \dot{x} = -\frac{(x-au)\sqrt{2b(\frac{xe^{-x}}{1-e^{-x}} - ln(\frac{xe^{-x}}{1-e^{-x}})-1)}}{S\kappa_e b(R_a+R_c)(1-\frac{1-e^{-x}}{xe^{-x}})\frac{e^{-x}(1-e^{-x}-x)}{(1-e^{-x})^2}} \\ y = \frac{3\alpha_0\kappa_e\sqrt{2b(\frac{xe^{-x}}{1-e^{-x}} - ln(\frac{xe^{-x}}{1-e^{-x}})-1)}}{aY_eH^2} + \Delta P \end{cases} \tag{11}$$

For the IPMC actuators, to ensure safety and longer service life of IPMC, and the process input is subject to a constraint on its magnitude. Considering uncertainties and input constraints, a nonlinear robust control design using operator-based robust right coprime factorization is studied, so that the validity of the obtained nonlinear model and the effectiveness of the proposed control method can be confirmed.

3 Robust stable control design using operator based approach

3.1 Operator theorem and robust right coprime factorization

Let X and Y be linear spaces over the field of real numbers, and let X_s and Y_s be normed linear subspaces, called the stable subspaces of X and Y, respectively, defined suitably by two normed linear spaces under certain norm $X_s = \{x \in X : \|x\| < \infty\}$ and $Y_s = \{y \in Y : \|y\| < \infty\}$. Generally, an operator $Q : X \to Y$ is said to be bounded input bounded output (BIBO) stable or simply stable if $Q(X_s) \subseteq Y_s$.

Definition 1. Let $S(X,Y)$ be the set of stable operators from X to Y. Then $S(X,Y)$ contains a subset defined by

$$u(X,Y) = \{M : M \in S(X,Y)\} \tag{12}$$

where, M is invertible with $M^{-1} \in S(Y,X)$. Elements of $u(X,Y)$ are called unimodular operators.

Next, generalized Lipschitz operator is introduced, which is defined on extended linear space. Thus, extended normed linear space, or simply, extended linear space is noted firstly.

Let Z be the family of real-valued measurable functions defined on $[0,\infty)$, which is a linear space. For each constant $T \in [0,\infty)$, let P_T be the Projection operator mapping from Z to another linear space, Z_T, of measurable functions such that

$$f_T(t) := P_T(f)(t) = \begin{cases} f(t), & t \le T \\ 0, & t > T \end{cases} \tag{13}$$

where, $f_T(t) \in Z_T$ is called the truncation of $f(t)$ with respect to T. Then, for any given Banach space X of measurable functions, set

$$X^e = \{f \in Z : \|f_T\|_X < \infty, \text{for all } T < \infty\} \tag{14}$$

Obviously, X^e is a linear subspace of Z. The space so defined is called the extended linear space associated with the Banach space X.

We note that the extended linear space is not complete in norm in general, and hence not a Banach space (complete normed vector space), but it is determined by a relative Banach space. The reason of using extended linear space is that all the control signals are finite time-duration in practice, and many useful techniques and results can be carried over from the standard Banach space X to the extended space X^e if the norm is suitably defined.

Definition 2. Let X^e and Y^e be extended linear spaces associating respectively with two given Banach spaces X and Y of measurable functions defined on the time domain $[0,\infty)$, and let D be a subset of X^e. A nonlinear operator $Q : D \to Y^e$ is called a generalized Lipschitz operator on D if there exists a constant L such that

$$\left\|[Q(x)]_T - [Q(\tilde{x})]_T\right\|_Y \le L\|x_T - \tilde{x}_T\|_X \tag{15}$$

for all $x, \tilde{x} \in D$ and for all $T \in [0,\infty)$. Note that the least such constant L is given by the norm of Q with

$$\begin{aligned} \|Q\|_{Lip} &:= \|Q(x_0)\|_Y + \|Q\| \\ &= \|Q(x_0)\|_Y + \sup_{T\in[0,\infty)} \sup_{\substack{x,\tilde{x}\in D \\ x_T \neq \tilde{x}_T}} \frac{\left\|[Q(x)]_T - [Q(\tilde{x})]_T\right\|_Y}{\|x_T - \tilde{x}_T\|_X} \end{aligned} \tag{16}$$

for any fixed $x_0 \in D$.

We remark that the family of standard Lipschitz operator and generalized Lipschitz operator are not comparable since they have different domains and ranges. The definition of generalized Lipschitz operator has been proved more useful than standard Lipschitz operator for nonlinear system control and engineering in the considerations of stability, robustness, uniqueness of internal control signals. For any operators defined throughout the paper, they are always assumed to be generalized Lipschitz operators. For simplicity, Lipschitz operator is always mean the one defined in generalized case in this paper.

Based on the concept of Lipschitz operator, an operator-based nonlinear feedback control system with uncertainty shown was considered in [5,6]. The nominal plant and uncertainty are P and ΔP, respectively, and the real plant $\tilde{P} = P + \Delta P$. The right factorization of the nominal plant P and the real plant $\tilde{P}$ are $P = ND^{-1}$, $P + \Delta P = (N + \Delta N)D^{-1}$, where N, ΔN, and D are stable operators, D is invertible, ΔN is unknown but the upper and lower bounds are known. Moreover, the factorization is said to be coprime, or P is said to have a right coprime factorization, if there exist two stable operators A and B satisfying the Bezout identity,

$$AN + BD = M \tag{17}$$

where, B is invertible, $M \in u(W,U)$ is unimodular operator. Under the condition of (17), if

$$\begin{cases} A(N+\Delta N) + BD = \tilde{M} \in u(W,U) \\ \|(A(N+\Delta N) - AN)M^{-1}\| < 1 \end{cases} \tag{18}$$

the BIBO stability of the nonlinear feedback control system with uncertainty can be guaranteed, that is, the system has the robust stability property, where, $\tilde{M} \in u(W,U)$ is unimodular operator, and $\|\cdot\|$ is Lipschitz operator norm.

It's worth to mention that the initial state should also be considered, that is, $AN(w_0,t_0) + BD(w_0,t_0) = M(w_0,t_0)$ should be satisfied. In this paper, $t_0 = 0$ and $w_0 = 0$ are selected.

3.2 Operator-based controllers design

Considering the nonlinear system with bounded uncertainties, the robust control problem by using robust right coprime factorization approach has been researched. Assume that the uncertainties are given as ΔP, where ΔP is unknown but bounded. The right factorization of the nonlinear system is the following form

$$\tilde{P} = P + \Delta P = (N + \Delta N)D^{-1} \tag{19}$$

From [11], we can see that if the following conditions are satisfied,

$$\begin{cases} AN + BD = L \\ A(N+\Delta N) + BD = \tilde{L} \\ \|(A(N+\Delta N) - AN)L^{-1}\| < 1 \end{cases} \tag{20}$$

then the stability of the uncertain system $\tilde{P}$ is guaranteed, where L and $\tilde{L}$ are unimodular operators and $\|\cdot\|$ is Lipschitz operator norm, and shown in Fig. 1.

Then, we consider the mentioned nonlinear IPMC control model by using robust right coprime factorization. For the model described by equation (11), there exist some uncertainties ΔP in the IPMC model. The uncertainties are unknown but bounded. In Fig. 1, the uncertainties can be transformed into uncertain operator ΔN. That is, uncertain operator ΔN denotes the uncertainties caused by approximate calculation.

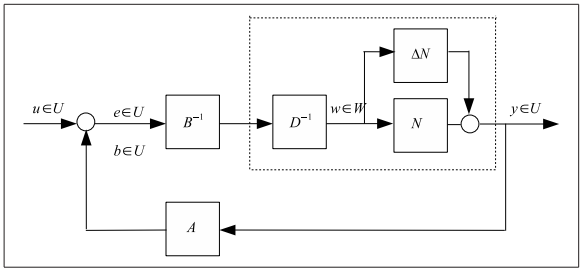

Fig. 1: A nonlinear system with uncertainties based on robust right coprime factorization

Denote N, D and ΔN as the following forms,

$$\begin{cases} D(\omega)(t) = \frac{S\kappa_e b(R_a+R_c)\dot{\omega}(t)(1-\frac{1-e^{-\omega(t)}}{\omega(t)e^{-\omega(t)}})\frac{e^{-\omega(t)}(1-e^{-\omega(t)}-\omega(t))}{(1-e^{-\omega(t)})^2}}{a\sqrt{2b(\frac{\omega(t)e^{-\omega(t)}}{1-e^{-\omega(t)}} - ln(\frac{\omega(t)e^{-\omega(t)}}{1-e^{-\omega(t)}}) - 1)}} \\ \qquad + \frac{\omega(t)}{a} \\ N(\omega)(t) = \frac{3\alpha_0\kappa_e\sqrt{2b(\frac{\omega(t)e^{-\omega(t)}}{1-e^{-\omega(t)}} - ln(\frac{\omega(t)e^{-\omega(t)}}{1-e^{-\omega(t)}}) - 1)}}{aY_eH^2} \\ \Delta N(\omega)(t) = \Delta\sqrt{2b(\frac{\omega(t)e^{-\omega(t)}}{1-e^{-\omega(t)}} - ln(\frac{\omega(t)e^{-\omega(t)}}{1-e^{-\omega(t)}}) - 1)} \end{cases} \tag{21}$$

To ensure safety and longer service life of IPMC, and the process input $u_d(t)$ is subject to the following constraint on its magnitude,

$$u_d(t) = \sigma(u_1(t))$$
$$\sigma(v) = \begin{cases} u_{max}, & v > u_{max} \\ v, & u_{min} \le v \le u_{max} \\ u_{min}, & v < u_{min} \end{cases} \tag{22}$$

where $u_1(t)$ is the control input before the constraint. u_{max} = 3V and u_{min} = -3V are maximum voltage and minimum voltage to ensure safe operation of the IPMC, respectively. When the input is limited in (22), the limited part can be equivalent to uncertainty of the system. Then, the entire uncertainty of the system is expressed as the following form

$$\Delta\tilde{N} : W \to Y$$

Then, we can design operators A and B to satisfy the following Bezout equations. If $-u_{max} \le u_1 \le u_{max}$,

$$\begin{cases} A_1N + BD = I \\ \|A_1(N+\Delta N) - A_1N)\| < 1 \end{cases} \tag{23}$$

else

$$\begin{cases} A_2N + BD = I \\ \|(A_2(N+\Delta\tilde{N}) - A_2N)\| < 1 \end{cases} \tag{24}$$

Where operator A_1 and A_2 is stable and B is invertible. Therefore, for the case of the IPMC control system with constraint inputs, we suppose that

$$B(u_d)(t) = au_d(t) \tag{25}$$

According to the robust stable conditions, if $-u_{max} \le u_1 \le u_{max}$,

$$A_1(y)(t) = -\frac{aSY_eH^2(R_a+R_c)}{3\alpha_0}\dot{y}(t) \tag{26}$$

else

$$A_2(y)(t) = -\frac{aSY_eH^2(R_a+R_c)}{3\alpha_0}\dot{y}(t)\phi(\sigma(u_1)) \tag{27}$$

where $\phi(\cdot)$ is constraint function related to $\sigma(u_1)$.

3.3 Tracking performance

Besides the robust stability of the IPMC system is guaranteed, the tracking performance of the system needs also to be considered. Here, the tracking condition is difficult to obtain for the operator N is a complex nonlinear function, such that we design a tracking system given in Fig. 2, where the stabilizing system regarded as the plant is equal to the system in Fig. 1. Here, the controller C is shown as the following form.

$$u(t) = K_p e(t) + K_i \int e(\tau)d\tau \tag{28}$$

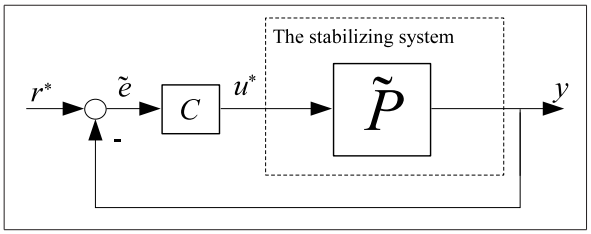

Fig. 2: The tracking control system

From Fig. 2, the error signal $\tilde{e}$ can be described in the following equation:

$$\tilde{e} = (I+\tilde{P}C)^{-1}(r^*) \tag{29}$$

where, I is the identity operator. Because the spaces of the nonlinear plant output Y and reference input U are the same, it is obvious that the operator $(I+\tilde{P}C)^{-1}$ is mapping Y to Y from Fig. 2. Hence, the relationship in the reference signal r^* and the error signal $\tilde{e}$ is in linear space. Then, one of conditions of the exponential iteration theorem is also satisfied, namely, the spaces of $\tilde{e}$ and y are the same. The designed controller C and the stabilizing system $\tilde{P}$ satisfy the following conditions.

1) For all t in $[0,\ T]$, C is stable, and $\tilde{P}(r^*) \ge K_1 > 0$ as $T \ge t \ge t_1 \ge 0$, $r^* > 0$.

2) $\tilde{P}C(0) = 0$.

3) $\|\tilde{P}C(x) - \tilde{P}C(y)\| \le h\int_0^t \|x-y, t_1\|dt_1$ for all x, y in the subspace Y_s of Y and for all t in $[0,\ T]$, h is any constant and is the gain of $\tilde{P}$ in the first norm, where the norm of x restricted to any interval $[0,\ T]$ will be denoted by $\|x,\ t\|$.

In this paper, the gain of $\tilde{P}$ is the generalized Lipschitz operator norm defined in *Definition* 2. Since C and $\tilde{P}$ are stable, the existence of h is ensured. Defining an operator from r^* to y as $\hat{G}$, we have $\hat{G} = \tilde{P}C * (I-\hat{G})$ as the feedback equation, where the cascade $\tilde{P}C * (I-\hat{G})$ means the operator $\hat{P}C$ following the operator $I-\hat{G}$. Then, we summarized the exponential iteration theorem in *Lemma* 1.

Lemma 1. (*Exponential Iteration Theorem*). The feedback equation $\hat{G} = \tilde{P}C * (I-\hat{G})$, in which all operators map the Banach space Y_B into itself, has a unique solution for $\hat{G}$, which converges uniformly on $[0,\ T]$, provided that conditions 2) and 3) are satisfied. The plant output is bounded [6].

Lemma 1 means since Y_s is complete the sequence is uniformly convergent on $[0,\ T]$. It may be established that $\hat{G} - \tilde{P}C * (I-\hat{G}) = 0$ and it is unique. Then the plant output is bounded. Further, $(I+\tilde{P}C)^{-1}(r^*)(t)$ exists.

Lemma 2. The error signal $\tilde{e}$ with the controller C can be made arbitrarily small. That is, $y(t) - r^*(t)$ can be made arbitrarily small by $t \le T$ large enough.

Proof. From Figs. 1 and 2, we have

$$y(t) = r^*(t) - \hat{e}(t) \tag{30}$$

From (29) and (30), we have

$$y(t) = r^*(t) - (I+\tilde{P}C)^{-1}(r^*)(t) \tag{31}$$

Since I is the identity operator, namely, $I(r^*) = r^*[1]$ [6], then

$$\begin{aligned} y(t) &= r^*(t) - (r^*(t) + \tilde{P}C(r^*(t)))^{-1} \\ &= r^*(t) - (r^*(t) + K_p\tilde{P}(r^*)(t) \\ &\quad + K_i\int_0^t \tilde{P}(r^*(\tau))d\tau)^{-1} \end{aligned} \tag{32}$$

Considering Condition 1) of the controller design, namely, $\tilde{P}(r^*) \ge K_1 > 0$ as $T \ge t \ge t_1 \ge 0$, we obtain

$$\begin{aligned} K_p\tilde{P}(r^*)(t) + K_i\int_0^t \tilde{P}(r^*(\tau))d\tau &\ge K_pK_1 + K_i\int_0^t \tilde{P}(r^*(\tau))d\tau)^{-1} \\ &\ge K_pK_1 + K_i\int_0^{t_1} \tilde{P}(r^*(\tau_1))d\tau_1 + K_iK_1\int_{t_1}^t d\tau_2 \end{aligned} \tag{33}$$

$K_iK_1\int_{t_1}^t d\tau_2$ can be made arbitrarily large by making $t < T$ large enough. Then, $(r^*(t) + K_p\tilde{P}(r^*)(t) + K_i\int_0^t \tilde{P}(r^*(\tau))d\tau)^{-1}$ becomes arbitrarily small. From (32), $y(t) - r^*(t)$ can be made arbitrarily small, and $y(t)$ tracks $r^*(t)$. This fact leads to the desired result, and the proof is completed.

From the analysis we can see that based on the proposed design scheme, the BIBO stability can be guaranteed by the designed operator controllers A and B. The output tracking performance can be realized by designed tracking controller C.

Table 1: Parameters in the IPMC

T	F	κ_e
290 K	96487 C mol^{-1}	$1.12\times10^{-6}Fm^{-1}$
R_a	R	Y_e
18 Ω	8.3143 J $mol^{-1}K^{-1}$	0.56 GPa
R_c	C^-	α_0
60 Ω	980 mol	0.12 J C^{-1}
L	W	H
50 mm	10 mm	200 μm

4 Simulation and experimental results

4.1 Experimental system

Fig. 3 shows photograph of experimental setup. In this experimental setup, an IPMC sample of dimensions 50 mm * 10 mm * 0.2 mm is clamped at one end, and is subject to voltage excitation generated from the computer and board (PCI-3521). A laser displacement sensor (ZX-LD40: 40±10mm) is used to measure the bending displacement d.

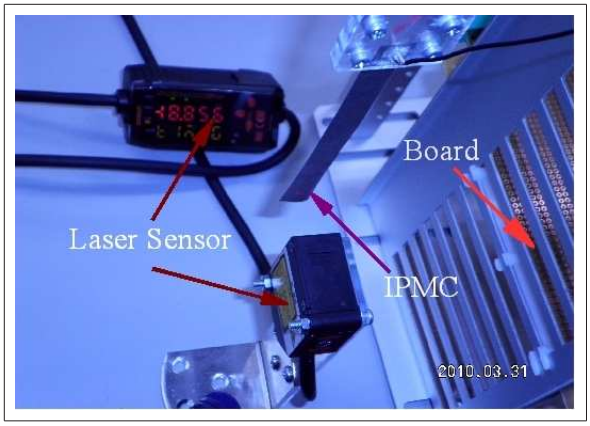

Fig. 3: Photograph of experimental setup

4.2 Simulation Results

Some identified physical parameters are shown in Table 1. In the simulation, the uncertain factor in (21) is modeled as $\Delta = \frac{3\alpha_0\kappa_e\sqrt{2b}}{aY_eh^2}\times5\%$. In fact, the uncertainties of model is smaller than ΔN, so robust stability of the system can be guaranteed. The curvature control simulation results of the IPMC based on right coprime factorization with uncertainties and without uncertainties are shown in Fig. 4, respectively. From Fig. 4, we can see the nonlinear IPMC with uncertainties system using right coprime factorization is robust stable. Fig. 5 shows the simulation result of system with tracking controller, the reference input of the curvature is $r_f = 1[1/m]$, where the tracking controller is given as follows.

$$u(t) = 50e(t) + 0.000015\int e(\tau)d\tau \tag{34}$$

From Fig. 5, we can find that the IPMC control output can track the reference input using the tracking controller.

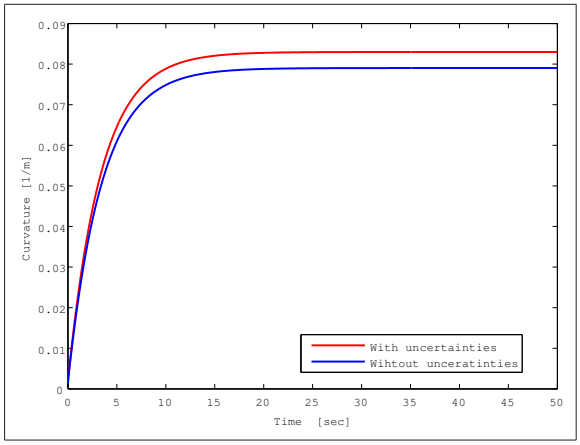

Fig. 4: The curvature control simulation results based on the proposed method

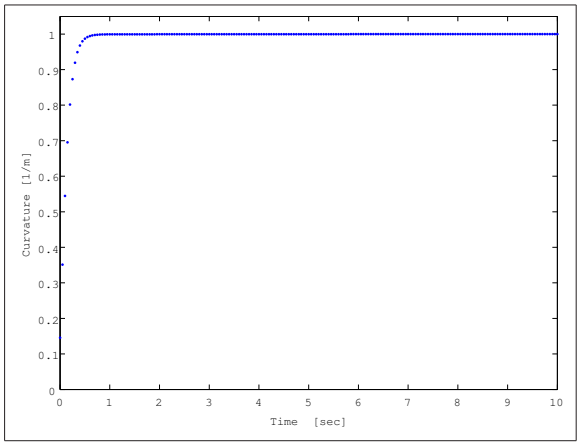

Fig. 5: The simulation result with tracking controller

4.3 Experimental result

Fig. 6 shows the displacement response, where the desired outputs of displacement d are 4 [mm], 8 [mm], 12 [mm], respectively. The results show that the robust stability of the IPMC displacement control system is guaranteed and tracking performance is satisfied by using the proposed method.

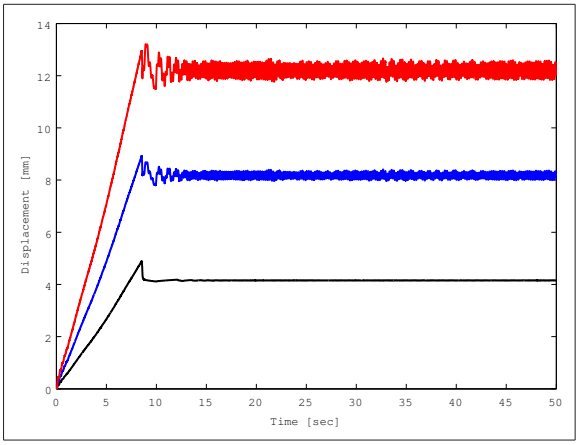

Fig. 6: Experimental result on output response

5 CONCLUSIONS

In this paper, we investigate robust nonlinear control for the IPMC with uncertainties and input constraints. The nonlinear model of the IPMC with uncertainties and input constraints is described. To avoid the influence of the uncertainties and input constraints, robust right coprime factorization approach for the IPMC displacement control system is proposed. Finally, simulation and experimental results are presented to show the effectiveness of the proposed method.

Acknowledgement

The authors would like to thank National Nature Science Foundation of China (61074022 and 61304115), and Program for International Science Cooperation and Communication (2010DFA22770) for their support of this work.

References

[1] M. Shahinpoor and K. Kim, Smart Mater. Struct., **10**, 819 (2001).
[2] M. Shahinpoor and K. Kim, Smart Mater. Struct., **13**, 1362 (2004).
[3] Z. Chen, D. R. Hedgepeth, and X. Tan, Smart Mater. Struct., **18**, 9 (2009).
[4] N. Bhat and W. Kim, J. Syst. Control Eng., **218**, 421 (2004).
[5] G. Chen and Z. Han, IEEE Trans. Automatic Control, **43**, 1505 (1998).
[6] M. Deng, A. Inoue and K. Ishikawa, IEEE Trans. Automatic Control, **51**, 645 (2006).
[7] M. Deng, S. Bi and A. Inoue, IET Control Theory & Applications, **3**, 1237 (2009).
[8] S. Bi and M. Deng, Int. J. Control, **84**, 815 (2011).
[9] A. Wang and M. Deng, Appl. Math. Inf. Sci., **6**, 459 (2012).

Aihui Wang received his B. S. and M. S. degrees in Control Theory and Control Engineering from Zhengzhou University, in 2001 and 2004, respectively. He received his Ph. D. in Electronic Engineering from Tokyo University of Agriculture and Technology, Japan, in 2012. From 2004 to 2009 he was with School of Electric and Information Engineering, Zhongyuan University of Technology, China, as a lecturer. He is currently an associate professor at School of Electric and Information Engineering, Zhongyuan University of Technology, China. His research interests include robust nonlinear control and bio-robot.

Gong Wei received his B. S. degree in computer science from Henan University in 1996. He received his M. S. degree in computer and application from Tianjin University in 2006. From 2008 he has been working in Department of Information Engineering of Henan Communication Vocational technology College, China. He is currently an associate professor at Department of Information Engineering of Henan Communication Vocational technology College, China. His research interests include computer control and complex system control.

Hui Wang received her B. S. degrees in Industrial Automation from North China Electric Power University in 2003, and received her M. S. degrees in Test and Measurement Technology and Instruments from Zhengzhou University in 2011. Since 2011, she was with School of Electric and Information Engineering, Zhongyuan University of Technology, China, as a lecturer. His research interests include robust nonlinear control and computer control.